Research Paper

Journal of Chemical Research

Journal of Chemical Research
July-August 1–15
© The Author(s) 2023
Article reuse guidelines:
sagepub.com/journals-permissions
DOI: 10.1177/17475198231184799
journals.sagepub.com/home/chl

Sage

M^{pro}-targeted anti-SARS-CoV-2 inhibitor-based drugs

Zhuxin She[1], Yinuo Yao[1], Conglong Wang[1], Yi Li[1], Xiaohui Xiong[1] and Yuanyuan Liu[2]

Abstract

The COVID-19 pandemic caused by severe acute respiratory syndrome coronavirus 2 is a global health emergency. The main protease is an important drug target in coronaviruses. It plays an important role in the processing of viral RNA-translated polyproteins and is highly conserved in the amino acid sequence and three-dimensional structure, making it a good drug target for which several small molecule inhibitors are available. This paper describes the various anti-severe acute respiratory syndrome coronavirus 2 inhibitor drugs targeting M^{pro} discovered since the severe acute respiratory syndrome coronavirus 2 outbreak at the end of 2019, with all these compounds inhibiting severe acute respiratory syndrome coronavirus 2 M^{pro} activity *in vitro*. This provides a reference for the development of severe acute respiratory syndrome coronavirus 2 M^{pro}-targeted inhibitors and the design of therapeutic approaches to address newly emerged severe acute respiratory syndrome coronavirus 2 mutant strains with immune evasion capabilities.

Keywords

covalent inhibitor, M^{pro}, non-covalent inhibitor, severe acute respiratory syndrome coronavirus 2, targeted inhibitor

Date received: 30 March 2023; accepted: 12 June 2023

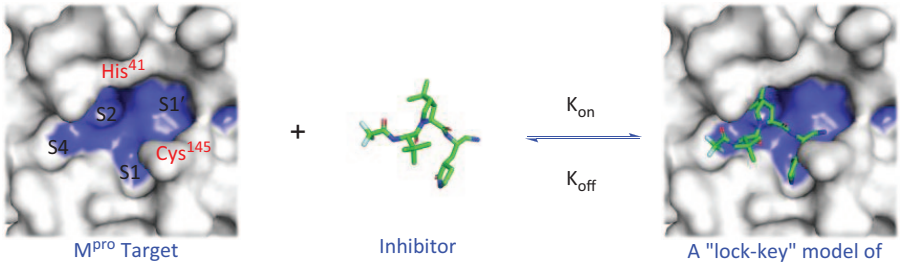

Introduction

Background

Since the outbreak of novel coronavirus pneumonia (COVID-19) in December 2019, the resulting global pandemic posed a huge threat to human life and health, and caused significant losses to the global economy. Therefore, it is urgent to develop effective prevention and treatment strategies.[1–3] The genome sequence of the pathogen of COVID-19 was first published on 11 January 2020. The pathogen was identified as a novel coronavirus (2019-nCoV), which was later named as severe acute respiratory syndrome coronavirus 2 (SARS-CoV-2) by the International Committee on Virus Taxonomy (ICTV).[4]

At present, the world is still fighting SARS-CoV-2 and has rapidly deployed effective vaccines to combat the pandemic.[5] Although many vaccines have been approved for the prevention of COVID-19, most COVID-19 vaccines were developed for the early pandemic strains, due to the

[1]College of Food Science and Light Industry, Nanjing Tech University, Nanjing, P.R. China
[2]School of Pharmaceutical and Chemical Engineering, ChengXian College, Southeast University, Nanjing, P.R. China

Corresponding authors:
Yi Li, College of Food Science and Light Industry, Nanjing Tech University, Nanjing 211816, P.R. China.
Email: liynj2012@njtech.edu.cn

Yuanyuan Liu, School of Pharmaceutical and Chemical Engineering, ChengXian College, Southeast University, Nanjing 210088, P.R. China.
Email: liuyuanyuan1985419@163.com

Creative Commons Non Commercial CC BY-NC: This article is distributed under the terms of the Creative Commons Attribution-NonCommercial 4.0 License (https://creativecommons.org/licenses/by-nc/4.0/) which permits non-commercial use, reproduction and distribution of the work without further permission provided the original work is attributed as specified on the SAGE and Open Access pages (https://us.sagepub.com/en-us/nam/open-access-at-sage).

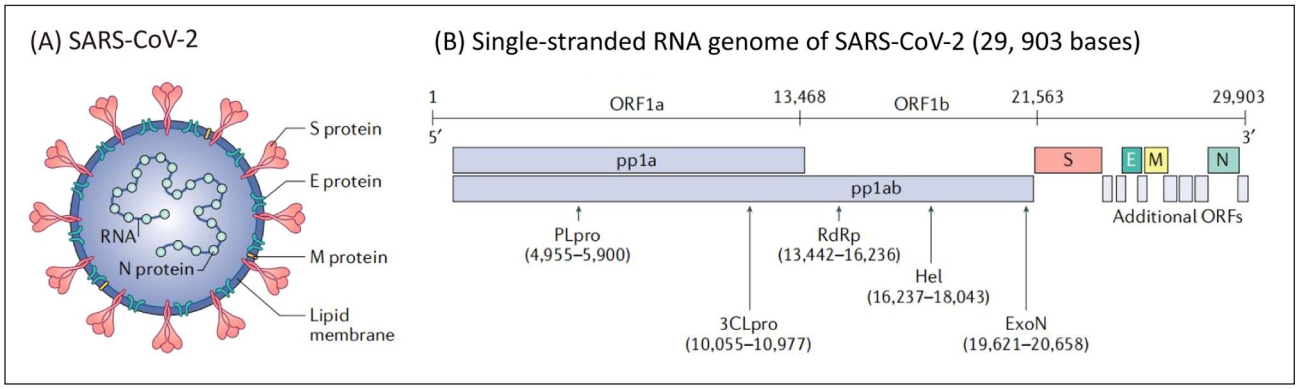

Figure 1. (a) Structure and (b) genomic composition of SARS-CoV-2.[2]

rapid and frequent variation of the virus, including the Alpha (B.1.1.7) variant, the Beta (B.1.351) variant, the Gamma (P.1) variant, the Delta (B.1.617.2) variant, and the Omicron (B.1.1.529) variant.[6] The low titer of the antibody leads to a shortening of the protection time of the vaccine, limited protection of the naturally acquired and vaccine-induced antibodies against infection by the Omicron variant strain, and the resurgence of SARS-CoV-2 infection in the highly vaccinated population, which impairs the efficacy of the vaccine.[7] Therefore, it is crucial to develop more effective specific drugs and treatment methods for more conservative viral targets to curb the spread of COVID-19 and reduce mortality.[8]

Biological basis of targeted SARS-CoV-2 M^{pro} treatment

SARS-CoV-2 is a positive single-stranded RNA virus with a genome of about 30,000 nucleotides. Genome sequencing shows that the genome sequence of this pathogenic coronavirus has 96% homology with that of bat coronavirus and belongs to the same genus as the pathogen SARS-CoV that caused the outbreak of SARS in 2003 β-coronavirus, with 89.1% nucleotide similarity and 79% homology.[9] The RNA genome of SARS-CoV-2 contains at least six open reading frames (ORFs), but the first ORF (ORF1a/b) accounts for about two-thirds of the length of the genome. It directly translates into two large overlapping precursor proteins pp1a and pp1ab (Figure 1). They must be cut and processed into functional subunits for replication and transcription activities.[10] The cleavage process is completed by two viral proteases: the main protease M^{pro} (also known as 3CL^{pro}) and the papain-like protease PL^{pro}, both of which are encoded by ORF1a, and these polyproteins are processed into 16 non-structural proteins (NSPs).[11] These NSPs are involved in the production of subgenomic RNA, encoding four main structural proteins (envelope (E) protein, membrane (M) protein, spike (S) protein, and nucleocapsid (N) protein), and other auxiliary proteins.[12] SARS-CoV-2 mainly infects host cells by binding with angiotensin-converting enzyme 2 (ACE2) on the surface of host cells through the receptor binding domain (RBD) of the S protein. Therefore, the hydrolysis of pp1a/pp1ab by proteolytic enzymes is an indispensable key step in the process of viral RNA replication and transcription, and plays a crucial role in the life cycle of COVID-19.

One of the most characteristic drug targets of coronavirus is the main protease M^{pro}, which is a chymotrypsin-like cysteine protease that exists in the non-structural protein 5 (NSP5) of the virus.[13] Like papain, this enzyme is essential for processing the multi-protein translated from the virus RNA.[14] M^{pro} is a cysteine protease with three domains (Domains I–III) (Figure 2), which is involved in most mature cleavage events in the precursor protein. M^{pro} is encoded by ORF1 as an NSP5. It cleaves the poly-protein pp1ab of the virus at 11 different positions, and the core cleavage motif is Leu-Gln↓(Ser/Ala/Gly).[15,16] The active site of M^{pro} contains a catalytic dimer composed of Cys^{145} and His^{41}. The catalytic dimer consists of four main pockets, which are marked according to their position relative to the shear bond of the substrate. The active site is located in the gap between the two N-terminal domains of the three domains of the monomer, while the C-terminal helical domain is involved in the regulation and dimerization of the enzyme.[10] Inhibiting M^{pro} activity will prevent virus replication, so M^{pro} protease is an important antiviral target.[13,17,18] Although there are many potential drug targets on SARS-CoV-2,[1,19–22] such as RNA-dependent RNA polymerase RdRp, spinous RBD, and glucose regulatory protein GRP78, M^{pro} only cleaves peptides after glutamine (Gln) residues, and the human body lacks its homologous protein enzyme.[23] Its structure has been verified by X-ray crystallography, and its active form is a homodimer.[10] The active center with less plasticity is mainly composed of His^{41} and Cys^{145}, which is relatively conservative in pathogenic β-coronaviruses and not easy to mutate,[24,25] so it becomes an ideal target for drug development against COVID-19.

Targeted inhibitors of SARS-CoV-2 main protease

From the perspective of the interaction mechanism of targeting M^{pro} targets, the reported SARS-CoV-2 M^{pro} inhibitors can be divided into two categories: One type is a covalent inhibitor that can bind to the active pocket of M^{pro}, and the groups on the compound react with the target site to form covalent bonds, thereby inhibiting its biological

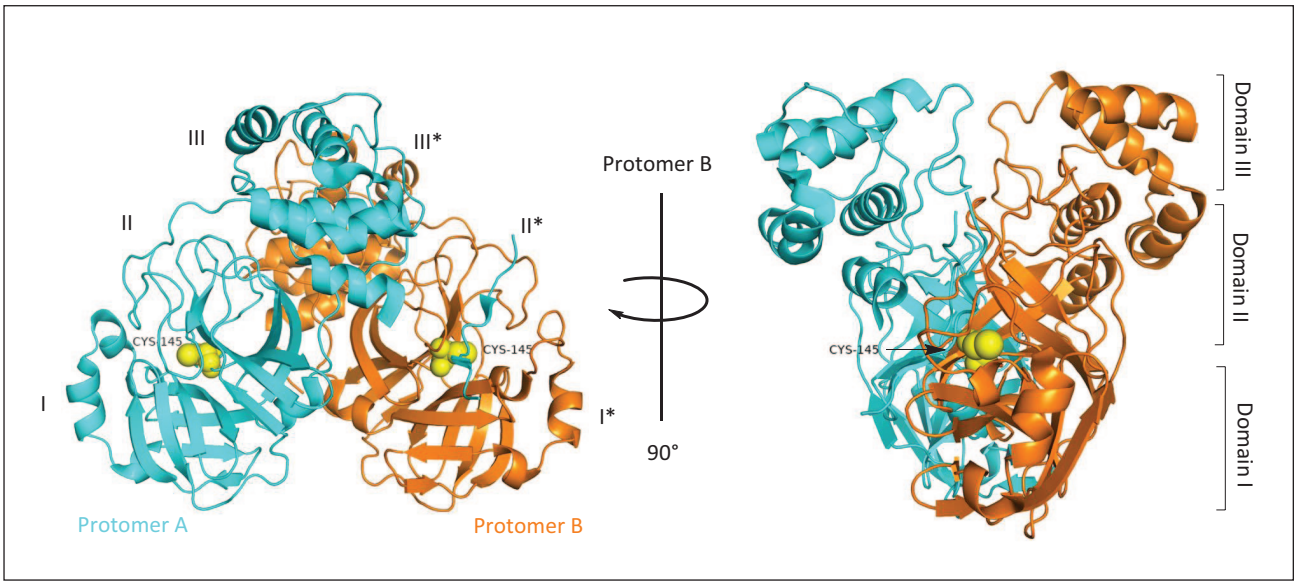

Figure 2. Three-dimensional structure of SARS-CoV-2 M^{pro} from two different perspectives.[15]

function. The other type is non-covalent inhibitors that use non-covalent interactions with binding pockets to reversibly bind to enzyme targets, while the inhibitors themselves do not react. The M^{pro} inhibitors reported in this paper were tested for their cytotoxicity against Vero E6, HPAEpiC, and A549 cells. Both *in vivo* and *in vitro* activity tests showed low/submicromolar activity, and examination of the pharmacokinetics also showed good oral absorption effects. This provides a reference for the rational design of more inhibitors and the discovery of candidate drugs for the treatment of COVID-19.

Covalent inhibitors

M^{pro} covalent inhibitors contain electrophilic warheads or connect electrophilic groups to modify known non-covalent ligand fragments. Cys^{145} is used as the anchor point of the electrophilic warhead for covalent binding, resulting in changes in protein conformation and playing an inhibitory role. The covalent bond formed with the target allows the inhibitor to have a high potential energy and a high coordination efficiency. In addition, it can prolong the duration of pharmacological action and lower the frequency of administration, thus potentially reducing the drug dosage to improve safety. According to the classification of electrophilic warheads, covalent inhibitors mainly include ketoamides, nitriles, sulfonates, Michael acceptors, aldehydes, and organic selenium compounds.

α-Ketoamides

The team of Rolf Hilgenfeld at the University of Lübeck designed, synthesized, and evaluated the inhibitory activity of several α-ketoamide peptidomimetic inhibitors against SARS-CoV-2 M^{pro}(compounds **1–4**) (Figure 3(a)).[15] To improve the half-life of **1** in plasma, the P3–P2 amide bond is hidden in a pyridone ring, preventing cellular proteases from entering the bond and lysing it, while replacing the hydrophobic cinnamoyl group with a slightly less hydrophobic Boc group which increases the solubility of this compound in plasma and reduces its binding to plasma proteins, leading to compound **2**. Compound **2** was optimized, and Compound **3** was obtained by replacing the P2 cyclohexyl of **2** with cyclopropyl and improved the antiviral activity against SARS-CoV-2. However, Compound **4**, obtained by removing the Boc group, showed a loss of activity and weakened inhibition, indicating that the Boc and hydrophobic groups were necessary for the interaction between M^{pro} and the cell membrane. Thus, the crystal structure of the SARS-CoV-2 M^{pro} complex with the α-ketoamide inhibitor **3** was reported (Figure 3(b)) and its lung tissue level was monitored (IC_{50} = 0.67 μM, EC_{50} = 1.75 μM).[15] The pharmacokinetic profiles demonstrate significant pulmonary tropism and suitability for administration via the inhalation route,[11] providing a useful framework for the development of anti-coronavirus drugs containing ketoamide inhibitors.

In May 2022, the team of Professor Lei Jian and Yang Shengyong of West China Hospital of Sichuan University reported a series of potent M^{pro} inhibitors **5** (Y180) (Figure 4(a)) containing an α-ketoamide and obtained using the Ugi four-component reaction (Ugi-4CR) (IC_{50} = 8.1 nM).[26] An acetyl group was introduced at the terminal acyl of the amide, which allowed the formation of an α-ketoamide warhead in the S1′ pocket. Furthermore, to reduce the epimerization of the most active epimer ((*R*)-epimer) to its less active epimer ((S)-configuration), deuterium was used to replace the exchangeable hydrogen attached to the chiral carbon linking the two amides (Figure 4(b)). Compound **5** is effective against wild-type SARS-CoV-2, B.1.1.7 (Alpha), B.1.617.1 (Kappa), and P.3 (Theta), with EC_{50} values of 11.4, 20.3, 34.4, and 23.7 nM, respectively. Oral treatment with **5** showed significant antiviral efficacy. It was also very effective against the B.1.1.529 (Omicron) variant *in vitro* and *in vivo*, significantly reducing the viral load, reducing tissue damage, and improving the survival

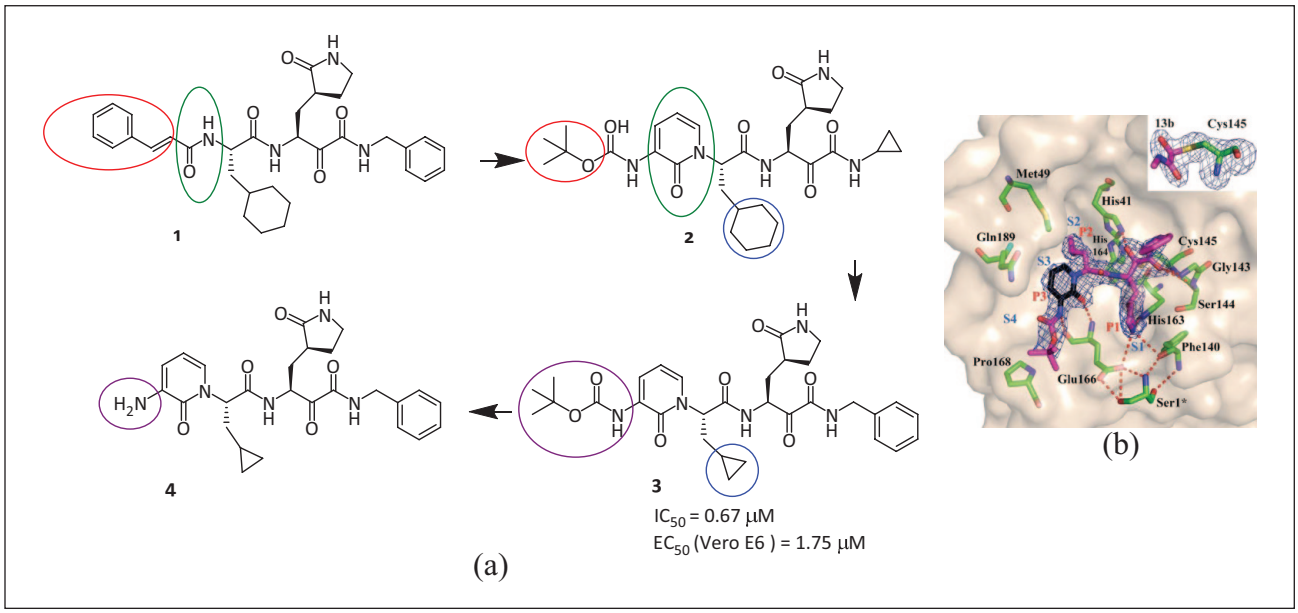

Figure 3. (a) Chemical structures of the inhibitors **1**–**4**; (b) crystal structure of **3** bound to the M^{pro} active site.[15]

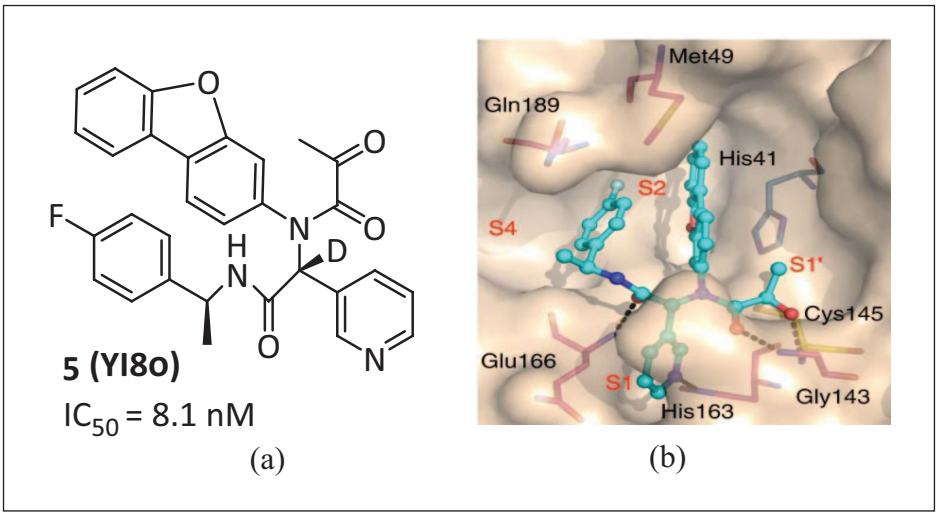

Figure 4. (a) Chemical structure of compound **5** and (b) detailed interactions of M^{pro} and compound **5**.[26]

rate of infected animals. The covalent bond formed with the target gives the inhibitor high potential energy and ligand efficiency, and can prolong the time of efficacy, lower the frequency of administration, and possibly reduce the drug dose, thus improving safety.

Compound **6** (Boceprevir; Figure 5(a)) is an FDA-approved serine protease inhibitor for the treatment of hepatitis C virus (HCV).[27] Its ketoamide group can covalently bind with Ser^{139} of HCV NS3 protease.[28] The drug can also inhibit M^{pro} enzyme activity with an IC_{50} value of 4.13 μM and an EC_{50} value of 1.90 μM for SARS-CoV-2.[29] In the M^{pro}–Boceprevir composite structure (PDB: 6ZRU and 7C6S), the nucleophilic Cys^{145} in M^{pro} forms a C–S covalent bond with the ketone carbon of **6**, the oxygen of the α-ketoamide in **6** forms H bonds with the Cys^{145} and Gly^{143} backbone chain amides, occupying oxygen anion holes, and the hydroxy group covalently added by the α-ketoamide forms hydrogen bonds with His^{41} of the side chain, both of which are stable conformations. The backbone of His^{164} and Glu^{166} forms an H bond with the amide bond on the backbone of compound **6**. The dimethylcyclopropyl moiety is inserted deep into the S2 pocket and forms extensive hydrophobic contacts with His^{41}, Met^{49}, Met^{165}, Asp^{187}, Arg^{188}, and Gln^{189}. The *tert*-butyl group is directed into the S4 pocket and is stabilized by several H bonds to the backbone oxygen of Glu^{166} and by hydrophobic interactions with the side chains of Met^{165}, Gln^{192}, Leu^{167}, and Pro^{168} (Figure 5(b)). Due to **6** being an approved drug for the treatment of HCV, there are a large number of data in terms of dose, toxicity, and pharmacokinetics, which can accelerate the research and development process of its use in SARS-CoV-2 treatment.

Nitriles

In September 2020, the Pfizer company reported compound **8** (PF-00835231) as a potent inhibitor of

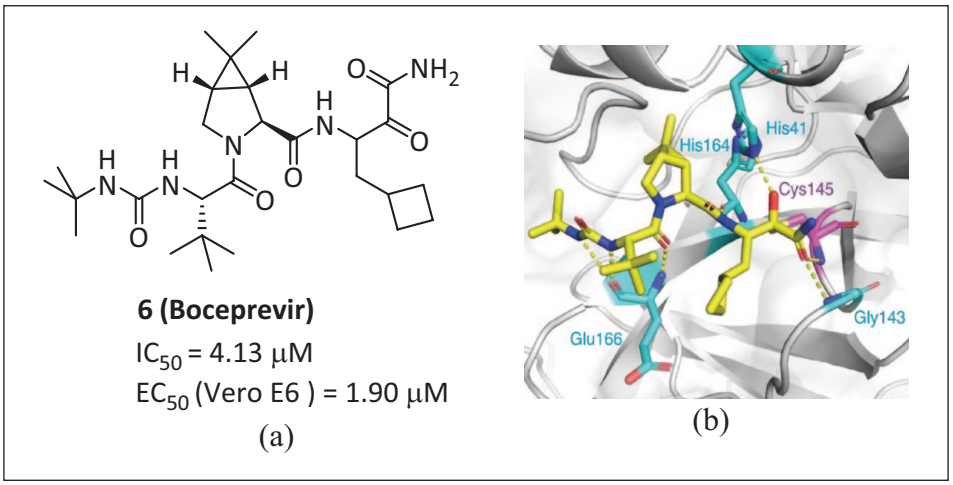

Figure 5. (a) Chemical structure of **6** and (b) the interaction diagram of M^{pro} and **6**.[30]

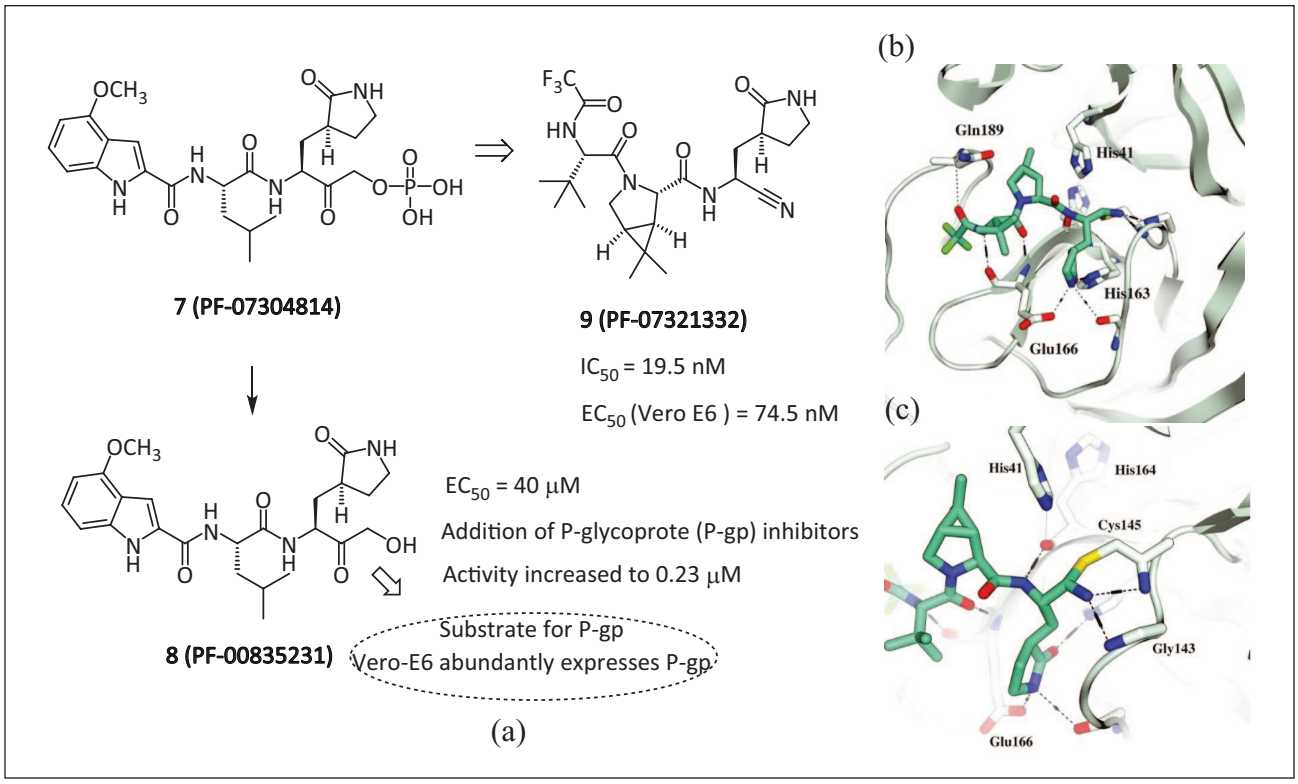

Figure 6. (a) Chemical structures of the inhibitors **7**, **8**, and **9**; (b) SARS-CoV-2 M^{pro}-bound crystal structure of **9**; and (c) a reversible covalent Cys^{145} adduct is formed with the nitrile substituent in **9**.[33]

SARS-CoV-2 M^{pro}.[31] This compound had been previously identified for the treatment of SARS-CoV, and given that SARS-CoV M^{pro} and SARS-CoV-2 M^{pro} have homology, it was repurposed. It is based on the phosphate prodrug **7** (PF-07304814) designed by Pfizer, which hydrolyzes into the active form **8** when administered in the body. The phosphate prodrug **7** was also described to increase the potential for the intravenous treatment of COVID-19.[32] However, **7** has to be administered intravenously, making it less appealing for massive distribution and relegating its use to hospital settings. Meanwhile, due to the polarity of **8**, it cannot be absorbed by the intestine through oral administration. Therefore, based on the modification of compound **7**, an oral M^{pro} inhibitor **9** (PF-07321332) was prepared (Figure 6(a)).[33]

Compound **9** (also called Nirmatrelvir) is a pseudo-peptide covalent inhibitor with a nitrile warhead. It can directly bind to the cysteine catalytic residue of the SARS-CoV-2 M^{pro} protein, and selectively and reversibly inhibit SARS-CoV-2 M^{pro} activity (IC_{50} = 19.5 nM, EC_{50} = 74.5 nM, Ki = 3.11 nM).[33,34] Compound **9** has similarities with the dimethylcyclopropylproline and *tert*-leucine groups of Boceprevir. The molecular simulation also shows that the interaction of inhibitor **9** is similar to that of Boceprevir, and the interaction of the pyrrolidone group with the H bond between Glu^{166} is similar to that of **8**. The eutectic

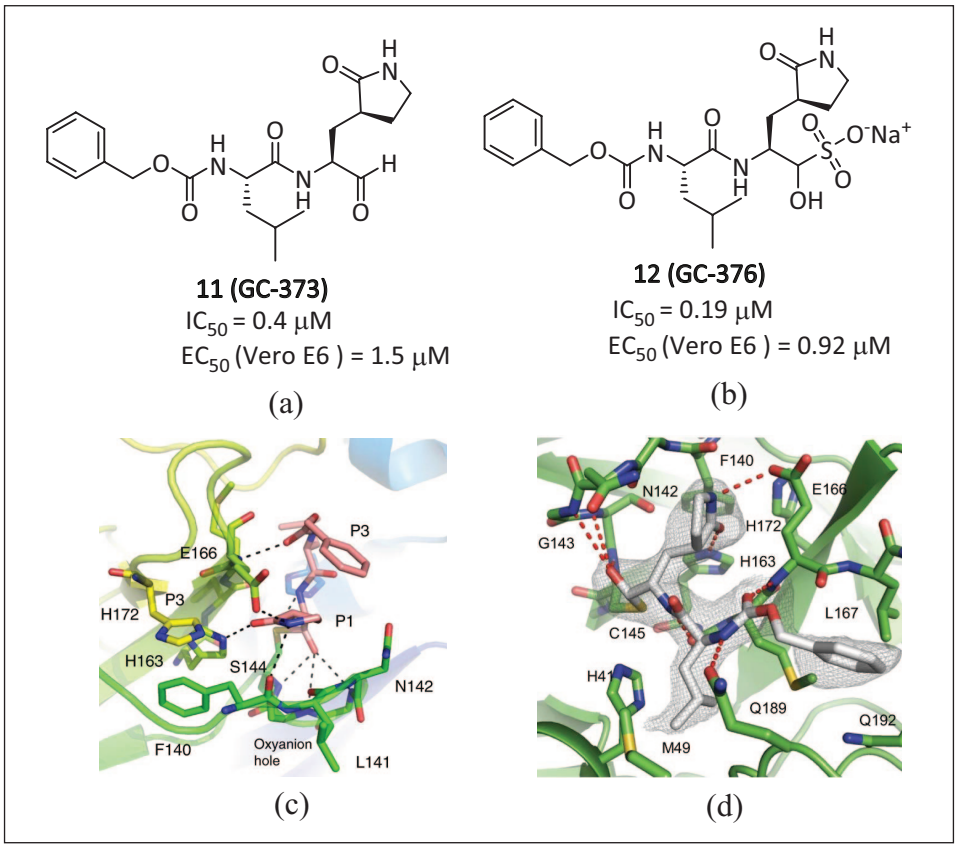

Figure 7. Chemical structures of the inhibitors (a) **11** and (b) **12** and the interaction diagrams of (c) **11** and (d) **12** with the active site complex of M^{pro}.[36,37]

structure of **9** (PDB: 7RFW) shows that the P1′ nitrile group of the inhibitor and the mercaptan group of Cys^{145} form a reversible covalent thioimidate and form two hydrogen bonds with Cys^{145} and Gly^{143}.[18] The bicyclic tetrahydropyrrole part and trifluoroacetyl group occupy the S2 and S4 pockets, respectively. The (S)-γ-lactam at the P1 site and the amide backbone at the P3–P4 site established multiple hydrogen bonds with His^{163}, Glu^{166}, and Gln^{189}, respectively (Figure 6(b)). The antiviral activity in mice showed that **9** could effectively reduce the viral load of SARS-CoV-2 in the lungs of mice and slow down the progression of the disease. In clinical trials involving healthy human participants, oral plasma concentrations exceeded *in vitro* antiviral cell efficacy.[33] A pharmacokinetic property study showed that the CYP3A4 enzyme oxidatively metabolizes multiple sites of **9** (e.g. *tert*-butyl, azabicyclic, and pyrrolidone), resulting in rapid clearance.

Ritonavir is a human immunodeficiency virus type 1 (HIV-1) protease inhibitor, which has no activity against SARS-CoV-2 M^{pro}. However, ritonavir can bind to the CYP3A4 enzyme to inhibit the metabolism of **9**. This increases the concentration of **9** in plasma and prevents its inactivation by liver metabolism. In December 2021, the US FDA approved compound **9** and the low-dose HIV antiviral drug ritonavir (CYP3A4 inhibitor) combined inhibitor PAXLOVID as the first oral antiviral drug for the treatment of COVID-19, which is intended to be administered in combination to treat and prevent COVID-19.[35]

Meanwhile, Pfizer is also working on the second-generation COVID-19 oral administration of compound **10** (PF-07817883). A phase I clinical trial (NCT05580003) was released in clinical trials to evaluate the safety and blood levels of **10** in healthy people. Currently, it has entered the phase II clinical trial (NCT05799495) to understand the effect and safety of the study medicine of **10** in adults. The new drug still selects the M^{pro} target, but its oral absorption effect is better than Paxlovid. Though similar to Paxlovid, the drug does not need to be administered in combination with ritonavir, as Paxlovid currently is. Compound **10** no longer requires ritonavir to prolong blood concentration, which could reduce the risk of interactions with other drugs. Pfizer has not spoken extensively about the program, and it did not come up at the company's J.P. Morgan presentation, though it was highlighted at a recent Pfizer investor event on the high-value pipeline of the company.

Sulfonates

Vuong et al. have described two types of peptide-like covalent inhibitors, namely parent **11** (GC-373; Figure 7(a)) and its prodrug **12** (GC-376; Figure 7(b)). These two drugs were previously used to treat feline infectious peritonitis (FIP) and showed good antiviral activity against the SARS-CoV-2 virus. The IC_{50} values are 0.40 and 0.19 μM, and the EC_{50} values are 1.5 and 0.92 μM, respectively.[36,37] The crystal structures and NMR analyses of SARS-CoV2 M^{pro} using **11** and **12** showed that the prodrug **12** was converted into the parent drug **11**, resulting in the covalent connection of the drug to Cys^{145} as a hemi-thioacetal, indicating that

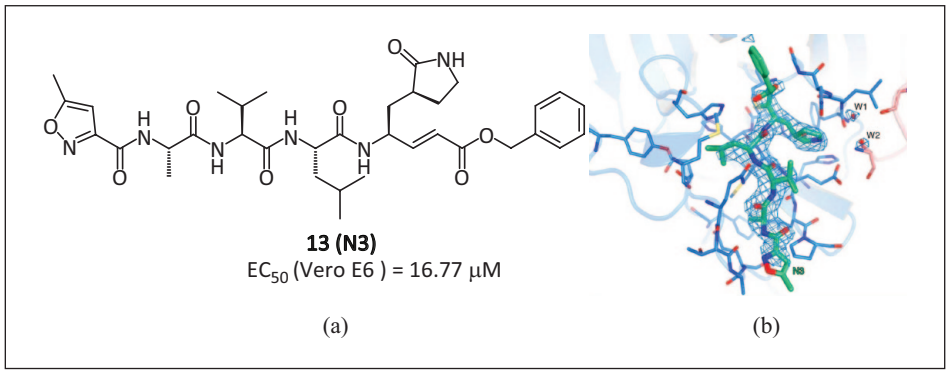

Figure 8. (a) The covalent inhibitor **13** containing the Michael acceptor and (b) its co-crystallization with M^{pro}.[41]

the bisulfite group had left **12**. The glutamine surrogate in the P1 position of **11** forms a hydrogen bond with the side chain of His^{163} and Glu^{166}, and a hydrophobic interaction with His^{172}. The carbonyl in P3 forms a hydrogen bond with the backbone amide of Glu^{166} (Figure 7(c)). The (S)-γ-lactam ring of the P1 part of **12** forms a hydrogen bond with the His^{163} and Glu^{166} side chains and the main chain of Phe^{140}, combined with the S1 site of M^{pro}.[38] The carbamate bond of **12** forms hydrogen bonds with the main chain of Glu^{166} and the side chain of Gln^{189}, connecting the isobutyl of P2 to the phenylmethyl ester interacting with the aliphatic S4 site, and the carbonyl group in P3 forms a hydrogen bond with the backbone amide of Glu^{166}, further stabilizing the binding of inhibitors (Figure 7(d)). Compared with the previous inhibitors, the phenylmethyl ester of **12** is highly complementary for the S4 site, and extensive nonpolar interactions may significantly improve the effectiveness of this compound. Compound **12** forms an extensive hydrogen bond network with active sites, making **12** one of the most effective SARS-CoV-2 M^{pro} inhibitors *in vitro*. Compound **12** has been proven to have more potent inhibition efficiency than Boceprevir.[30] In cell cultures, **11** and **12** can block virus replication and are non-toxic, which makes them more advantageous than Boceprevir in clinical practice. However, the side effects demonstrated by **12** in the tests may limit its use.[39,40]

Michael acceptor

The team of Yang Haitao and Rao Zihe and that of Jiang Hualiang used computer-aided drug design to determine a potential inhibitor **13** (N3) (Figure 1(a)) for the main protease M^{pro} of SARS-CoV-2,[41] which contains a Michael acceptor as a warhead and can effectively fight against a variety of coronaviruses, including SARS-CoV and the Middle East respiratory syndrome coronavirus (MERS-CoV).[42] Compound **13** has antiviral effects in SARS-CoV-2-infected Vero cells (EC_{50} = 16.77 μM). The crystal structure of the complex of SARS-CoV-2 M^{pro} and inhibitor **13** was analyzed (PDB 6LU7). The β–C atom on the α,β-unsaturated ester of **13** forms a covalent bond (1.8 Å C–S distance) with Cys^{145} (Figure 8(b)), indicating that a Michael addition reaction has occurred, confirming that compound **13** is a Michael-type inhibitor. In addition, the lactam occupies the S1 pocket and forms a hydrogen bond with His^{163}, and the isobutyl of the Leu side chain is inserted into the S2 pocket. The side chain of Val of P3 is exposed, indicating that these parts may not be the key to inhibiting the activity. The structure of these parts can be optimized to improve the efficacy and pharmacokinetic characteristics. The Ala side chain on the P4 side is inserted into the S4 pocket to form a small hydrophobic pocket together with the surrounding amino acids, which also helps to lock the inhibitor in the substrate-binding pocket.

Aldehydes

The Chinese Academy of Sciences and Shanghai University of Science and Technology jointly designed and synthesized two SARS-CoV-2 M^{pro} peptide covalent inhibitors **14** and **15** with an aldehyde group as the warhead.[11] Both compounds have good antiviral activity. The IC_{50} values measured by the fluorescence resonance energy transfer (FRET) method are 53 and 40 nM. In Vero-E6 cells, the EC_{50} values of SARS-CoV-2 are 0.53 and 0.72 μM, respectively. The eutectic structures of **14** and **15** with SARS-CoV-2 M^{pro} (Figure 9) show that the aldehyde group as an electrophilic group forms a covalent bond with the mercaptan group of Cys^{145}. The (S)-γ-lactam ring and indole-2-formyl group occupy the S1 and S4 pockets, respectively, and establish multiple hydrogen bonds with His^{163} and Glu^{166}. The cyclohexyl group of **14** and the 3-fluorophenyl group of **15** occupy the S2 pocket and form important hydrophobic interactions, in which the fluorine atom of the phenyl further establishes a hydrogen bond with Gln^{189}. Due to its good pharmacokinetic characteristics and low toxicity, **14** has now entered clinical research (Clinical trial No. NCT04766931). Compound **14** was later transferred to Frontier Biotechnologies Inc. and named FB2001. It is administered through atomization inhalation and now has entered into phase II/III clinical trials (NCT05675072).

Qiao et al.[23] synthesized 32 new small molecular compounds containing bicyclic proline fragments through rational drug design, which can effectively inhibit the activity of SARS-CoV-2 M^{pro} *in vitro* (IC_{50} 7.6–748.5 nM). The eutectic structure of the most active compound **16** (MI-23, IC_{50} = 7.6 nM) and M^{pro} reveal the interaction mode (Figure 10(a) and (b)). The carbon of the warhead aldehyde interacts with the sulfur atom of the catalytic residue Cys^{145} to form a 1.8 Å covalent bond, and the oxygen of the aldehyde

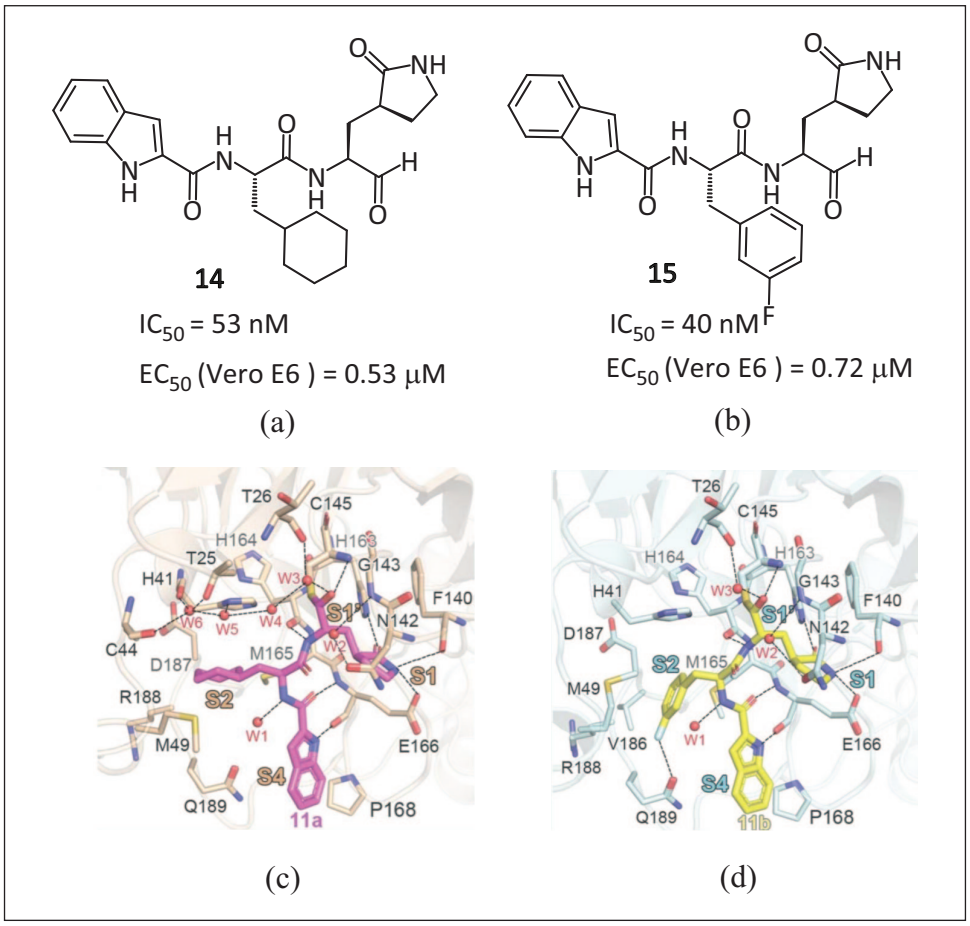

Figure 9. Chemical structures of inhibitors (a) **14** and (b) **15**; close-up view of (c) **14** and (d) **15** combined with M^{pro} pocket.[11]

interacts with the main chain amide of Cys^{145} and Gly^{143} to form two hydrogen bonds. The (S)-γ-lactam ring of P1 is deeply inserted into the S1 pocket, forming two hydrogen bonds with the side chain of His^{163} (2.8 Å) and the main chain of Phe^{140} (3.3 Å). The rigid P2 bicyclic proline group points to a hydrophobic S2 pocket and forms hydrophobic interactions with Met^{165}, Gln^{189}, His^{41}, Met^{49}, Asp^{187}, and Arg^{188}. The main chain oxygen of P3 interacts with the main chain amide of Glu^{166} through a 2.9 Å hydrogen bond, and the 1-ethyl-3,5-difluorobenzene part assumes an extended conformation and occupies the S4 site, and forms a multiple hydrophobic interaction with the residue of the catalytic pocket. Two compounds **17** (MI-09) and **18** (MI-30) with high activity, good pharmacokinetic properties, and safety showed excellent antiviral activity in transgenic mice infected with SARS-CoV-2 (Figure 10(c) and (d)). Oral or intraperitoneal injection can significantly reduce the lung viral load and lung pathological damage, and has the potential to develop anti-SARS-CoV-2 drugs.

Organic selenium compounds

Compound **19** (Ebselen) (Figure 11(a)) is an organoselenium molecule that can function as a glutathione peroxidase and peroxiredoxin mimic.[43] It has been shown to form a seleno-sulfide bond with thiol groups of cysteine (Cys) in a number of proteins which results in anti-inflammatory, antimicrobial, and neuroprotective effects.[44] Compound **19** has extremely low cytotoxicity (when administered orally; the median lethal dose of rats is more than 4600 mg kg^{-1}), and its safety to humans has been evaluated in many clinical trials.[45,46] Compound **19** was identified as a SARS-CoV-2 M^{pro} inhibitor in high-throughput screening with an IC_{50} value of 0.67 μM.[36] Amporndanai et al.[44] evaluated the inhibitory effect of Ebselen derivatives on SARS-CoV-2 M^{pro}, two of which showed a greater inhibitory effect on SARS-CoV-2 replication. From the eutectic study of M^{pro}-Ebselen and another effective compound (MR6-31-2), it was found that these compounds combine at M^{pro}-catalytic sites, form covalent bonds by providing selenium atoms, and block the His–Cys catalytic binary to inhibit M^{pro}-activity and virus replication (Figure 11(b)). Compound **19** and its derivatives have been proved to be effective in inhibiting papain-like protease (PL^{pro}), which is another key protease in inhibiting SARS-CoV-2 replication.[47] This dual inhibition of the two key enzymes of virus replication may be the reason for the effective antiviral effect of Ebselen, which has an important guiding role in the development of virus double-target inhibitors.

Non-covalent inhibitors

Although the covalent bond formed by an electrophilic warhead in a covalent inhibitor and the amino acid residues in the active pocket of the target protein can help to prolong the action time of a drug *in vivo*, it usually has potential toxic

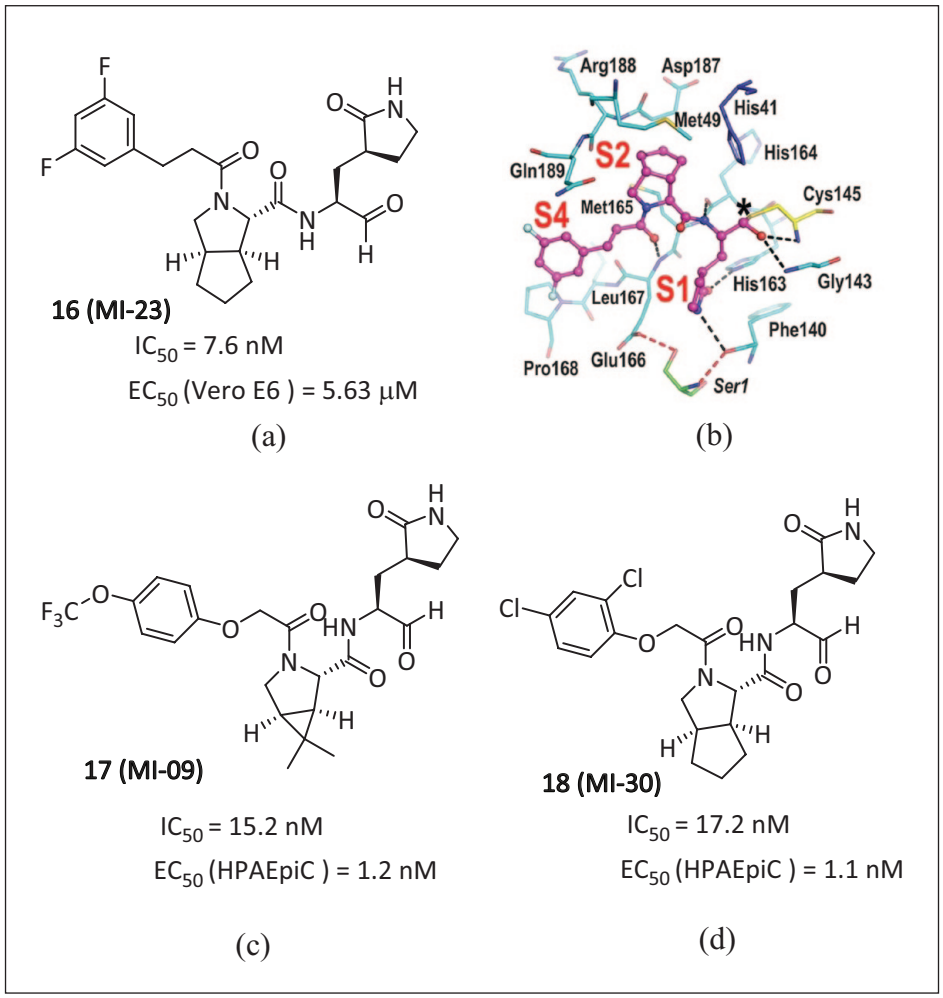

Figure 10. (a) Chemical structure of **16**; (b) interaction between M^{pro} and **16**; chemical structures of (c) **17** and (d) **18**.[23]

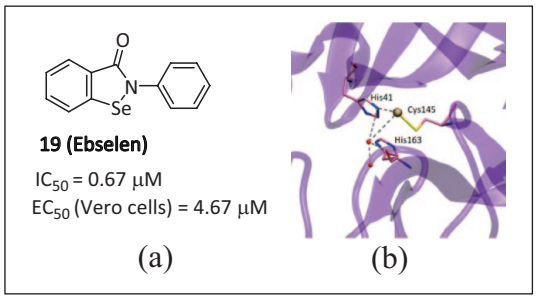

Figure 11. (a) Chemical structure of the inhibitor **19** and (b) details of the crystal structure of the selenium-M^{pro} complex.[48]

side effects and targeting problems. Non-covalent inhibitors that competitively bind to target proteins through weak reversible binding can greatly reduce these risks. Therefore, compared with covalent compounds, non-covalent inhibitors may have a higher selectivity for M^{pro}.[49,50]

S-217622

Compound **20** (S-217622) (Figure 2(a)) is the first non-covalent, non-peptide SARS-CoV-2 M^{pro} inhibitor with oral activity (IC_{50} = 13 nM). In April 2022, Shionogi Pharmaceutical Research Center released part of the phase II/III clinical trial data of its oral SARS-CoV-2 M^{pro} inhibitor **20**, which was used to treat COVID-19, at the ECCMID conference.[51] The data showed that it was well tolerated and effective against the Omicron strain. On 22 November 2022, Japan's Shionogi Pharmaceutical announced that the emergency use authorization of **20** had been approved by the Japanese Pharmaceutical and Medical Devices Agency (PMDA). This approval was based on the clinical phase II/III test results of the drug and was used for COVID-19 infected people above 12 years old. The IC_{50} value of the biochemical activity of **20** is 0.013 μM. The antiviral activity EC_{50} value is 0.37 μM. Human and rat liver microsomes have high metabolic stabilities of 96% and 88%, a high oral absorption rate of 97%, and a low clearance rate.

Figure 12(b) shows the X-ray co-crystal structure (PDB: 7VU6) of M^{pro} complexed with **20**. In the S1 site, the 1-methyl-1H-1,2,4-triazole unit fits into the S1 pocket, forming a hydrogen bond with the sidechain NH of His^{163}. The distinctive His^{41} flip was maintained in the complex, and the 2,4,5-trifluorobenzylic moiety occupied the hydrophobic S2 pocket and stacked with the side chain of His^{41}. The P1′ ligand, 6-chloro-2-methyl-2H-indazole moiety, entered into hydrogen bonding with the Thr^{26} mainchain NH and a hydrophobic contact with Met^{49}. A variety of interactions and a high degree of fit with the catalytic

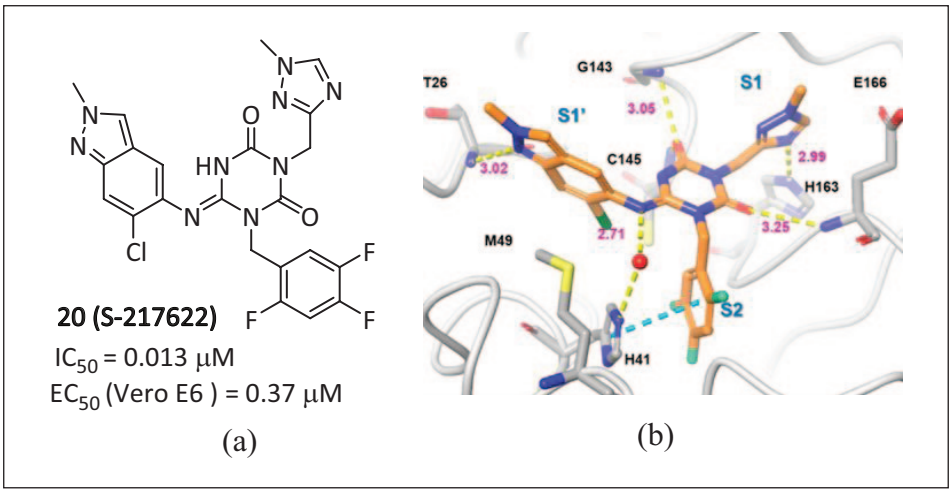

Figure 12. (a) Chemical structure of the inhibitor **20**; (b) X-ray eutectic structure of **20** with M^{pro}.[51]

pocket result in **20** having excellent inhibitory activity against M^{pro}. In addition, compound **20** showed a high level of inhibition against different virus strains (Alpha–Omicron), which dose-dependently inhibited the replication of SARS-CoV-2 in the lungs of mice. It can quickly reduce the viral load and shorten the time for viral titer to turn negative, with good tolerance.[52] Compared with **9**, compound **20** is expected to remove the dependence on P450 enzyme inhibitors and achieve single-drug treatment of COVID-19.

MCULE-5948770040 and HL-3-68

Clyde of the National Virtual Biotechnology Laboratory (NVBL) of the United States and others discovered a new non-covalent small molecule inhibitor **21** (MCULE-5948770040) (Figure 13(a)) that acts on the main protease of SARS-CoV-2, via high-throughput virtual screening (HTVS) and a targeted compound library (IC_{50} = 0.68 μM, Ki = 2.9 μM).[53] By resolving its room-temperature X-ray crystal structure at 1.8 Å (Figure 13(c)), compound **21** was found to be bound to a cleft in the active site of M^{pro}. It occupies subsites S1 and S2, forming stable hydrogen bonds and hydrophobic interactions. The uracil P1 group of the ligand is located on the S1 substituent driven by polarity, with the dichlorobenzene substituent of P2 occupying most of the hydrophobic S2 substituent. Furthermore, the position of the P2-dichlorobenzene group is stabilized by π–π stacking interactions with Gln^{189} and the imidazole side chain of catalytic His^{41}, with an interatomic distance of ~3.8 Å. The binding of **21** to the M^{pro} active site crack led to the overturn of the His^{41} side chain and the rotation of the χ^2 angle, creating a favorable geometric structure for π–π stacking with P2-dichlorobenzene in the complex structure. Molecular dynamics simulations illustrate that the interaction between ligands and M^{pro} changes the conformation state of M^{pro}, and points toward a mechanism of complementary interaction and inter-domain movement, including the proximal and distal movement of binding sites.

Kneller et al.[54] optimized the structure of **21** and obtained **22** (HL-3-68) (Figure 13(b)), which has a stronger inhibitory effect on SARS-CoV-2 M^{pro} than **21**, with an IC_{50} value of 0.29 μM. Through structure–activity relationship (SAR) studies, it was found that **22** stabilized the main interaction by "locking" the S1 and S2 sites, thus greatly reducing the flexibility of the loop around the main binding sites. The eutectic of **22** and M^{pro} further shows that the S2 pocket is very sensitive to minor changes in ligand properties (Figure 13(d)). A chlorine atom is introduced at the fifth position of the phenyl group, which makes Met^{49} rotate to accommodate additional chlorine atoms. It has a Van der Waals interaction with Cys^{44}, which enhances the combination with M^{pro}. Molecular dynamics (MD) simulations of the M^{pro}-HL-3-68 complex shows that the ligand **22** can stably bind to M^{pro}, forming a stronger interaction than **21**. SAR research analyzed the binding of non-covalent ligands and elucidated new details of M^{pro} as a drug target. This process provides a scalable framework for the further design of M^{pro} non-covalent inhibitors and the rapid discovery of feasible lead molecules targeting SARS-CoV-2.

Masitinib

Professor Savas Tay's team at the University of Chicago screened a library of 1900 clinically safe drugs against OC43, a human beta coronavirus that causes the common cold, and evaluated the top hits against SARS-CoV-2. They discovered that oral bioavailable tyrosine kinase inhibitor **23** (Masitinib) (Figure 14(a)) can effectively inhibit the activity of SARS-CoV-2 M^{pro} (IC_{50} = 2.5 μM, IC_{50} = 2.5 μM).[55] When compound **23** was used to treat mice infected with SARS-CoV-2, the virus titer in the lung and nasal cavity decreased by more than 200 times, the lung inflammation was reduced, and it was also effective for all variant strains tested *in vitro* (including B.1.1.7, B.1.351, and P.1). The co-crystal of **23** and SARS-CoV-2 M^{pro}(Figure 14(b)) shows that **23** is non-covalently bound to the catalytic pocket between the domains I and II of M^{pro} and blocks the key catalytic residues of the two active sites in the dimer. The pyridine ring has hydrophobic and Van der Waals interactions with the residue around the pocket, and is inserted into the S1 pocket to form a hydrogen bond

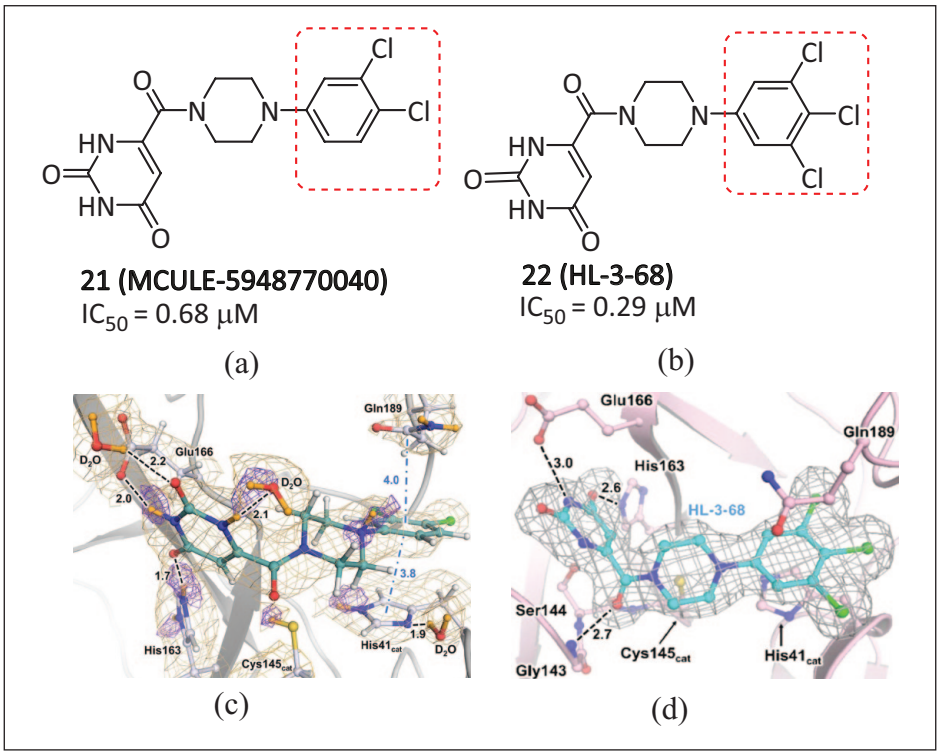

Figure 13. The chemical structures of (a) **21** and (b) **22**; X-ray crystal structures of M^{pro} complexed with (c) **21** and (d) **22**.[54]

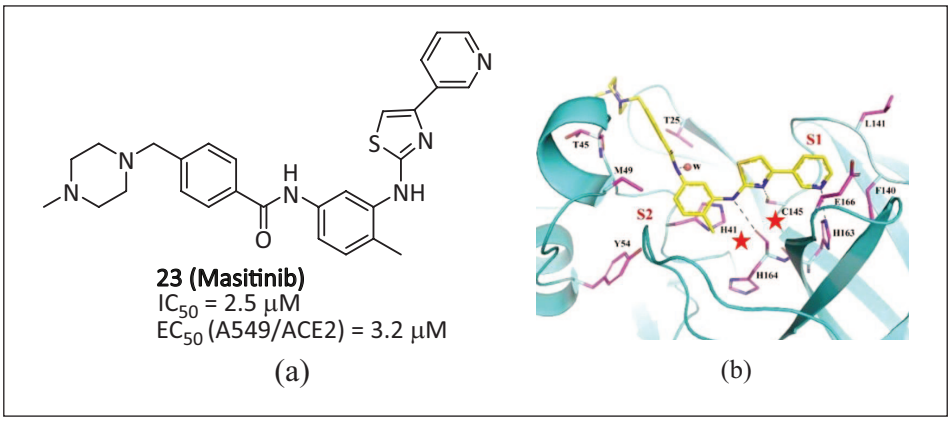

Figure 14. (a) Chemical structure of **23**; (b) band diagram of **23** interacting with M^{pro} at the active site, with the two catalytic residues marked with red stars.[55]

with His[163]. The aminothiazole ring forms two hydrogen bonds with His[164] and the key residue Cys[145]. The hydrophobic toluene ring occupies the S2 pocket and forms an important π–π stacking interaction with His[41]. The *N*-methylpiperazine group is located outside the catalytic pocket, and the absence of **23** is observed in the S1′ and S4 pockets, indicating that structural optimization can be carried out in these places to further improve the inhibitory activity of M^{pro} while reducing the inhibitory activity of tyrosine kinase and reducing the related side effects.[42]

ML188 and 23R

Compound **24** (ML188) (Figure 15(a)) is a non-covalent inhibitor aimed at SARS-COV-1 M^{pro} (IC_{50} = 1.5 μM, EC_{50} = 12.9 μM).[56] Lockbaum et al.[57] described the characteristics of the complex of SARS-CoV-2 M^{pro} and non-covalent inhibitor **24**, and solved the eutectic structure of the complex of **24** and SARS2-M^{pro} (Figure 15(c)) with a resolution of 2.39 Å. The interaction between protease and the inhibitor is through Van der Waals forces, and the SARS2-M^{pro}-ML188 force is −62.0 kcal mol^{-1}. Compared with SARS1-M^{pro}, non-covalent inhibitor **24** has a stronger binding effect on SARS2-M^{pro}. The complex of these two proteases is very similar, but the slight difference may lead to the higher efficacy of **24** against SARS2-M^{pro}, which indicates that **24** may provide a scaffold for a powerful non-covalent pan-coronavirus inhibitor.

Kitamura et al.[49] discovered a non-covalent small molecule inhibitor **25** (23R) (Figure 15(b)) based on the co-crystallization of GC376, calpain inhibitors XII, and ML188 (R) with M^{pro} using structural drug design and an

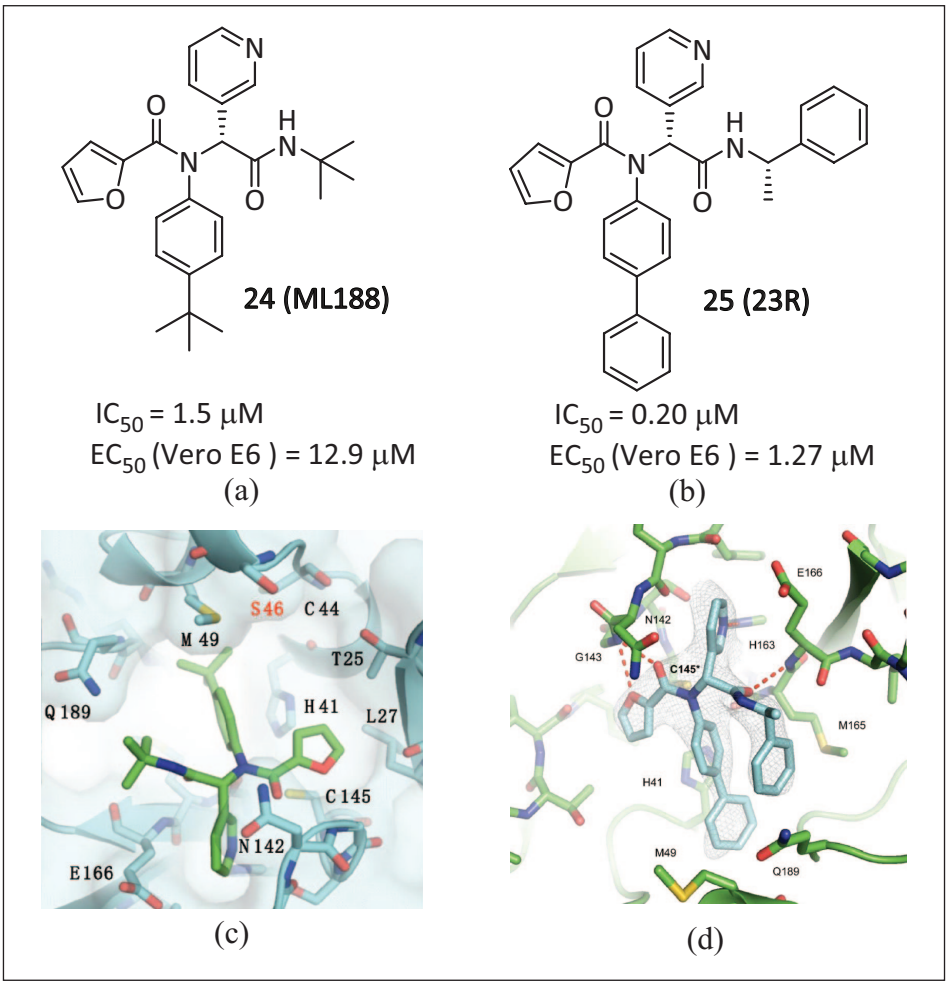

Figure 15. The chemical structures of (a) **24** and (b) **25**; co-crystal structure of M^{pro} in complex with (c) **24** and (d) **25**.[57,49]

Ugi-4CR methodology. It has high selectivity for host proteases, effective enzymatic inhibition, and antiviral activity *in vitro*. The IC_{50} value of SARS-CoV-2 M^{pro} in Vero E6 cells is 0.20 μM and the EC_{50} value is 1.27 μM. The X-ray crystal structure of SARS-CoV-2 M^{pro} in complex with **25** (Figure 15(d)) revealed a ligand-induced binding pocket between the S2 and S4 pockets, in which the benzyl ring from the terminal α-methylbenzyl fits in a pocket. This conformation is strengthened by π-stacking interactions with the first phenyl group of the biphenyl substituent. The benzyl ring is inserted into this binding pocket, strengthening binding with M^{pro}. This new binding mode of **25** was characterized by continuous intramolecular π-stacking, in which the phenyl group was clamped by furanyl and benzyl groups, contributing to its potent inhibition of M^{pro} with a favorable mechanism of action and robust cellular antiviral activity.

CCF0058981

Han et al.[58] from Cleveland University in the United States conducted a series of structural optimizations on the M^{pro} inhibitor ML300 of SARS-CoV-1. The non-covalent small molecule inhibitor **26** (CCF0058981) (Figure 16(a)) (IC_{50} = 68 nM) of SARS-CoV-2 was ultimately determined, making significant progress compared to the original SARS-CoV-1 ML300-derived inhibitors.[59] Investigation of the 3-chlorophenyl $P2_{sp}$ analogue of **27** (Figure 16(b)) afforded **26**. Substituting the 3-thienyl group of **27** with a 3-chlorophenyl moiety resulted of a significantly increased inhibitory effect. Compound **26** exhibited potent antiviral activity with EC_{50} values of 0.497 and 0.558 μM against SARS-CoV-2-infected Vero E6 cells in the cytopathic effect (CPE) inhibition assay and plaque reduction assay, respectively, being submicromolar in both assays, and thus achieving strong nanomolar biochemical inhibition of SARS-CoV-2 M^{pro}, submicromolar antiviral efficacy against SARS-CoV-2 live virus, and inhibition of plaque formation. The EC_{50}/IC_{50} ratio of **26** is 7.4, which is a high ratio among current M^{pro} non-covalent inhibitors. Its curative effect is equivalent to that of the clinical RNA polymerase inhibitor Remdesivir. The optimization of this series of compounds is currently underway, focusing on improving the Drug Metabolism and Pharmacokinetics (DMPK) profile and strong inhibition of CYP enzymes, with the aim of further improving the biochemical and cellular efficacy, and providing a direction for optimizing the structure of future inhibitors.

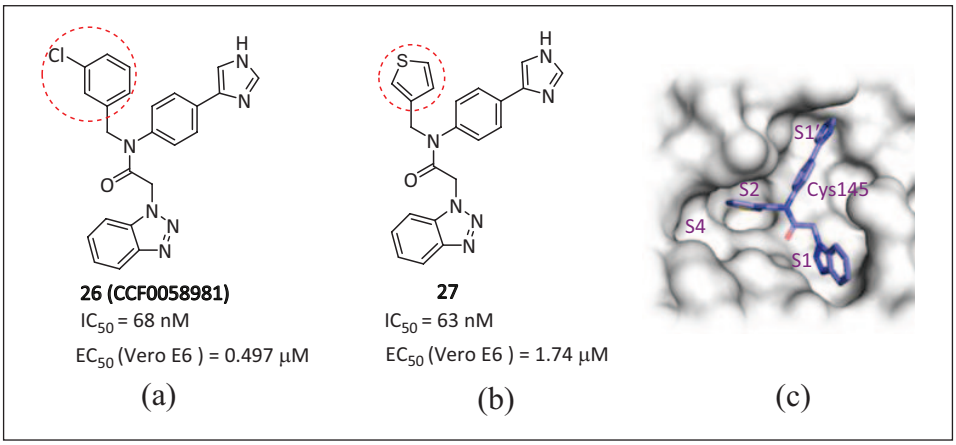

Figure 16. Chemical structures of (a) **26** and (b) **27**; (c) binding diagram of **26** in the M^{pro} activity pocket.[58]

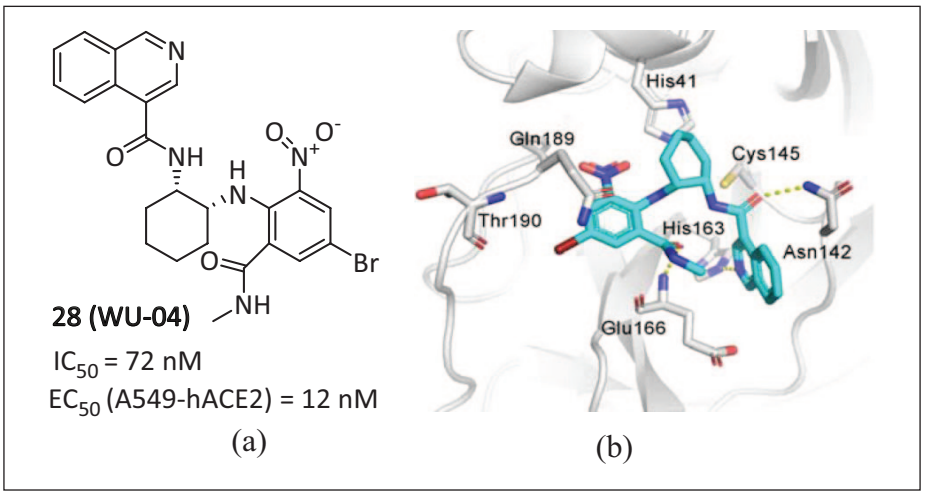

Figure 17. Chemical structure of (a) **28**; (b) interaction of **28** with M^{pro}.[60]

WU-04 (Mprosevir)

Recently, a non-covalent small molecule SARS-CoV-2 M^{pro} inhibitor **28** (WU-04) (Figure 17(a)), with an IC_{50} value of 72 nM and an EC_{50} value of 12 nM against SARS-CoV-2 in A549-hACE2 cells was discovered by the research team at West Lake University through DNA-encoded Library (DEL) technology screening.[60] The co-crystalline display of **28** with M^{pro} (Figure 17(b)) shows that the isoquinoline rings are well inserted into the S1 pocket and form hydrogen bonds with His^{163}. The carbonyl group at the 3-position of the isoquinoline ring and the methylcarbamoyl group form two hydrogen bonds with Asn^{142} and Glu^{166}. The phenyl ring and Gln^{189} form an amino–π interaction, and the 4-Br of the phenyl ring extends into the S4 pocket and establishes a halogen bond with Thr^{190}. The presence of a strongly electron-withdrawing 6-nitro group that reaches the S2 pocket is significant as it boosts the potency by strengthening both amino–π and the halogen bond interactions. Therefore, replacing the nitro group with other electron-withdrawing groups or hydrogen results in a decline or absence of inhibitory activity, which can be attributed to this key factor. The ability of **28** to inhibit SARS-CoV-2 replication was evaluated by the mouse model, and the efficacy of **28** *in vivo* was verified. *In vivo* antiviral activity showed that **28** exhibited anti-SARS-CoV-2 activity similar to that of PF-07321332 in K18-hACE2 mice when the same dose was administered orally. At present, compound **28** has completed preclinical studies on pharmacokinetics, efficacy, pharmacology, and safety evaluation, and was officially approved by the Center for Drug Evaluation (NMPA) to enter clinical practice in China.

Conclusion and Outlook

SARS-CoV-2 is still spreading and mutating around the world, damaging public health. The highly conserved main protease-targeting sequence has attracted more and more attention from researchers. In recent years, many types of SARS-CoV-2 M^{pro} inhibitors have been reported. The most common are covalent inhibitors that contain electrophilic warheads and take part in covalent binding with Cys^{145}. Due to the existence of highly reactive electrophilic warheads, the covalent inhibitors have potential safety problems of targeting and the disadvantages of poor oral bioavailability. Non-covalent small molecule inhibitors show inhibitory activity mainly through a weak reversible

interaction with the amino acid residues in the M^{pro}-catalytic pocket, but the lack of a strong interaction with the M^{pro}-catalytic pocket may lead to the need to extend the administration time or increase the dosage, which may lead to drug resistance. Therefore, non-covalent inhibitors that combine the characteristics of small molecules and the advantages of covalent inhibitor warheads may have a better potential for drug formation, but the currently reported inhibitors are few or have not entered the clinical trial stage.

Although many drugs have shown promising results in the fight against SARS-CoV-2, further validation is needed to determine whether these drugs pose risks due to the relatively short research periods. In addition, some examples have poor oral absorption effects,[61] high prices, and have side effects caused by drug–drug interactions.[62] As the clinical trials of ordinary COVID-19 patients did not meet expectations,[63] more clinical trials are needed to verify the safety and effectiveness of these drugs. Therefore, researchers still need to make continuous efforts to develop more powerful anti-SARS-CoV-2 inhibitors to cope with the emerging SARS-CoV-2 variants with immune escape function.

Since no known cysteine protease in the human body has the same cleavage site as M^{pro} and lacks its homologous protease, this indicates that in addition to M^{pro}-targeted inhibitors, it will be a promising direction to use protein degradation targeted chimerism (PROTAC) technology to develop degradation agents targeting the M^{pro} catalytic pocket as anti-coronavirus drugs. It is expected that in the near future, there will be more efficient M^{pro} inhibitors reasonably designed based on existing structures and using established technical means, and the development of new and powerful anti-coronavirus drugs will also benefit the discovery of other drug targets.

Declaration of conflicting interests

The author(s) declared no potential conflicts of interest with respect to the research, authorship, and/or publication of this article.

Funding

The author(s) disclosed receipt of the following financial support for the research, authorship, and/or publication of this article: This work was supported by the Natural Science Foundation of Jiangsu Province (Grant No. BK20211001), the Young and Middle-aged Academic Leaders of Jiangsu Province Youth and Blue Project (2021), and the National Research Project Incubation Fund of Chengxian College, Southeast University (Grant No. 2022NCF001). We are grateful to the High Performance Computing Center of Nanjing Tech University for supporting the computational resources.

ORCID iDs

Zhuxin She https://orcid.org/0009-0000-5186-4202
Yi Li https://orcid.org/0000-0002-0906-2799

References

1. Mhatre S, Srivastava T, Naik S, et al. *Phytomedicine* 2021; 85, 153286.
2. Perico L, Benigni A, Casiraghi F, et al. *Nat Rev Nephrol* 2021; 17: 46–64.
3. Lu RG, WU J, Bai X, et al. *Chin J Virol* 2020; 36: 927–935.
4. Wang XB, Wang A, Qu LL, et al. *J Agric Food Chem* 2020; 68: 14426–14437.
5. Tregoning JS, Flight KE, Higham SL, et al. *Nat Rev Immunol* 2021; 21: 626–636.
6. Shao WH, Chen XR, Zheng CF, et al. *Emerg Microbes Infec* 2022; 11: 2383–2392.
7. Keehner J, Horton LE, Binkin NJ, et al. *New Engl J Med* 2021; 385: 1330–1332.
8. Zhao Y, Fang C, Zhang Q, et al. *Protein Cell* 2022; 13: 689–693.
9. Lu RJ, Zhao X, Li J, et al. *Lancet* 2020; 395: 565–574.
10. Gunther S, Reinke PYA, Fernandez-Garcia Y, et al. *Science* 2021; 372: 642–646.
11. Dai WH, Zhang B, Jiang XM, et al. *Science* 2020; 368: 1331–1335.
12. Ramajayam R, Tan KP and Liang PH. *Biochem Soc T* 2011; 39: 1371–1375.
13. Anand K, Ziebuhr J, Wadhwani P, et al. *Science* 2003; 300: 1763–1767.
14. Hilgenfeld R. *Febs J* 2014; 281: 4085–4096.
15. Zhang LL, Lin DZ, Sun XYY, et al. *Science* 2020; 368: 409–412.
16. Knoops K, Kikkert M, van den Worm SHE, et al. *Plos Biol* 2008; 6: 1957–1974.
17. Zhang LL, Lin DZ, Kusov Y, et al. *J Med Chem* 2020; 63: 4562–4578.
18. Pillaiyar T, Manickam M, Namasivayam V, et al. *J Med Chem* 2016; 59: 6595–6628.
19. Ibrahim IM, Abdelmalek DH, Elshahat ME, et al. *J Infection* 2020; 80: 554–562.
20. Xia S, Liu MQ, Wang C, et al. *Cell Res* 2020; 30: 343–355.
21. Li TT, Han XJ, Gu CJ, et al. *Nat Commun* 2021; 12: 1–11.
22. Yan RH, Zhang YY, Li YN, et al. *Science* 2020; 367: 1444–1448.
23. Qiao JX, Li YS, Zeng R, et al. *Science* 2021; 371: 1374–1378.
24. Zhang DK, Chen J, Deng LB, et al. *Infect Genet Evol* 2010; 10: 84–88.
25. Goyal B and Goyal D. *ACS Comb Sci* 2020; 22: 297–305.
26. Quan BX, Shuai HP, Xia AJ, et al. *Nat Microbiol* 2022; 7: 716–725.
27. Tomei L, Failla C, Santolini E, et al. *J Virol* 1993; 67: 4017–4026.
28. Malcolm BA, Liu R, Lahser F, et al. *Antimicrob Agents Ch* 2006; 50: 1013–1020.
29. Oerlemans R, Ruiz-Moreno AJ, Cong YY, et al. *RSC Med Chem* 2021; 12: 370–379.
30. Fu LF, Ye F, Feng Y, et al. *Nat Commun* 2020; 11: 4417.
31. Hoffman RL, Kania RS, Brothers MA, et al. *J Med Chem* 2020; 63: 12725–12747.
32. Boras B, Jones RM, Anson BJ, et al. *Nat Commun* 2021; 12: 6055.
33. Owen DR, Allerton CMN, Anderson AS, et al. *Science* 2021; 374: 1586–1593.
34. Lamb YN. *Drugs* 2022; 82: 585–591.
35. Catlin NR, Bowman CJ, Campion SN, et al. *Reprod Toxicol* 2022; 108: 56–61.
36. Ma CL, Sacco MD, Hurst B, et al. *Cell Res* 2020; 30: 678–692.
37. Vuong W, Khan MB, Fischer C, et al. *Nat Commun* 2020; 11, 5409.
38. He XY, Zhen HY, Wu PY, et al. *Chin J Med Chem* 2021; 31: 301–311.
39. Pedersen NC, Kim Y, Liu HW, et al. *J Feline Med Surg* 2018; 20: 378–392.

40. Kim Y, Liu HW, Kankanamalage ACG, et al. *Plos Pathogens* 2016; 12: e1005531.
41. Jin ZM, Du XY, Xu YC, et al. *Nature* 2020; 582: 289–293.
42. Chen RF, Gao YL, Liu H, et al. *RSC Med Chem* 2023; 14: 9–21.
43. Nogueira CW, Barbosa NV and Rocha JBT. *Arch Toxicol* 2021; 95: 1179–1226.
44. Amporndanai K, Meng XL, Shang WJ, et al. *Nat Commun* 2021; 12: 3061.
45. Masaki C, Sharpley AL, Cooper CM, et al. *Psychopharmacology* 2016; 233: 2655–2661.
46. Kil J, Lobarinas E, Spankovich C, et al. *Lancet* 2017; 390: 969–979.
47. Weglarz-Tomczak E, Tomczak JM, Talma M, et al. *Sci Rep-UK* 2021; 11: 3640.
48. Agost-Beltran L, de la Hoz-Rodriguez S, Bou-Iserte L, et al. *Molecules* 2022; 27: 2523.
49. Kitamura N, Sacco MD, Ma CL, et al. *J Med Chem* 2022; 65: 2848–2865.
50. Zhang CH, Stone EA, Deshmukh M, et al. *ACS Central Sci* 2021; 7: 467–475.
51. Unoh Y, Uehara S, Nakahara K, et al. *J Med Chem* 2022; 65: 6499–6512.
52. Chen G, Guo H and Zhang F. *Chin J Pharm* 2022; 53: 763–774.
53. Clyde A, Galanie S, Kneller DW, et al. *J Chem Inf Model* 2022; 62: 116–128.
54. Kneller DW, Li H, Galanie S, et al. *J Med Chem* 2021; 64: 17366–17383.
55. Drayman N, DeMarco JK, Jones KA, et al. *Science* 2021; 373: 931–936.
56. Jacobs J, Grum-Tokars V, Zhou Y, et al. *J Med Chem* 2013; 56: 534–546.
57. Lockbaum GJ, Reyes AC, Lee JM, et al. *Viruses-Basel* 2021; 13, 174.
58. Han SH, Goins CM, Arya T, et al. *J Med Chem* 2022; 65: 2880–2904.
59. Turlington M, Chun A, Tomar S, et al. *Bioorg Med Chem Lett* 2013; 23: 6172–6177.
60. Hou NK, Shuai L, Zhang LJ, et al. *ACS Cent Sci* 2023; 9: 217–227.
61. Sendi P, Razonable RR, Nelson SB, et al. *Clin Microbiol Infec* 2022; 28: 1230–1235.
62. Marzolini C, Kuritzkes DR, Marra F, et al. *Ann Intern Med* 2022; 175: 744–747.
63. Zhang R and Mylonakis E. *Ann Intern Med* 2021; 174: JC17–JC17.